



In-situ synthesis of silica nanoparticle modified PVDF hydrophobic microporous membrane

Lingming La^{a,b}, Chenyu Den^a, Yuanbin Mo^a, Yanyue Lu^{a,*}

^aGuangxi Key Laboratory for Polysaccharide Materials and Modifications, School of Chemistry and Chemical Engineering of Guangxi University for Nationalities, Key Laboratory of Chemical and Biological Transformation Process of Guangxi Higher Education Institutes, Guangxi, Nanning 530006, China, emails: luyanyue@163.com (Y. Lu), lalingmin0429@163.com (L. La), 1107729613@qq.com (C. Den), 674148582@qq.com (Y. Mo)

^bSchool of Institute of New Carbon Materials, Taiyuan University of Technology, Shanxi, Taiyuan 030024, China

Received 17 August 2019; Accepted 25 January 2020

ABSTRACT

Nano-silica (nSiO₂) was synthesized in-situ by sol-gel method, then a (polyvinylidene fluoride) PVDF-nSiO₂ hydrophobic microporous composite membrane was prepared by mixing nSiO₂ sol into casting solution using non-solvent phase inversion. The effect of nSiO₂ sol addition on the surface and cross-sectional structure of the membrane, porosity, average pore size, pure water flux, membrane flux, and hydrophobic properties was investigated. Compared with the microporous membrane without nSiO₂ sol, the cross-sectional structure of the PVDF-nSiO₂ composite membrane is fully developed, the porosity is higher, the average pore diameter is larger, and the hydrophobicity is stronger. The direct contact membrane distillation (DCMD) experiment was carried out using the prepared composite membrane to simulate seawater desalination with a 30 g/L sodium chloride solution as feed solution. Compared with the microporous membrane without nSiO₂ sol added, the membrane flux was greatly improved to 31.02 kg m⁻² h⁻¹, and the porosity of the membrane was 75%. On the previous basis, the double coagulation bath method was employed to further improve the film-forming process. The properties and structure of the composite membrane were optimized. The membrane flux was 42.7 kg m⁻² h⁻¹, the porosity was 78.7%, and the contact angle was 127.3°. The performance of composite membrane was greatly improved.

Keywords: In-situ synthesis; Non-solvent phase inversion; Direct contact membrane distillation; Double coagulation bath method

1. Introduction

Membrane distillation [1–6] is a multi-scientific, efficient technology, and can be applied to various aspects such as seawater desalination [7–9], food industry [10–12], wastewater treatment [13], etc. It is a widely used separation technology. The concept of membrane distillation was proposed by Bodell in a patent in the 1860 s, but because the technical conditions were not very advanced at the time, it was greatly limited, and various research results were not satisfactory at that time. It was not until the 1980 s that it

began to develop, showing its practical potential. After the new century, it has been applied in many fields, especially in the separation of various aqueous solutions. In the membrane distillation process, the vaporization pressure difference formed by the temperature difference between the two sides of the hydrophobic membrane pushes the hot side water vapor to the cold side to purify the concentrated hot side solution. So the process does not need to be carried out under high temperature and high pressure. It can be carried out smoothly under conditions higher than

* Corresponding author.

normal temperature, which greatly saves costs. Therefore, it is possible to use energy sources such as solar energy, industrial waste heat, and geothermal energy, which are widely sourced and environmentally friendly, as their power source. Membrane distillation is an energy-saving and efficient separation technology. Its large-scale industrial development will greatly help to solve the problems of the environment, resources, and energy that human beings face today. However, the problem with membrane distillation is that the membrane used has a low membrane flux [14,15] and poor hydrophobicity.

With the rapid development of science and technology in the new century and the continuous development of this field, the membranes suitable for the membrane distillation process have been continuously developed. Francis et al. [9] used membrane distillation technology to successfully extract fresh water from red pigment with a membrane flux of $10.2 \text{ kg m}^{-2} \text{ h}^{-1}$, which did not achieve the desired results. Kamrani et al. [15] established a mathematical model of DCMD to investigate the effects of temperature, concentration, and flow rate on membrane flux.

Related studies [16–22] have shown that the addition of additives can change the phase transition rate of the film during film formation, thereby affecting the structure and properties of the film. For example, when an organic polymer is used as an additive, it affects the dispersion state of the solvent and the polymer in the casting solution. So that the non-solvent resistance of the casting solution is lowered, and the gel precipitation speed of the film is accelerated to cause instantaneous phase separation. As a result, it would increase the porosity of the membrane. When inorganic salts and inorganic oxides are used as additives, an ion-dipole acts between the high molecular polymer and the metal ions in the casting solution, and the non-solvent is trapped by the liquid film during phase inversion, and the solvent rapidly leaves the liquid film, so a large number of network pores formed to improve the permeability of the film. When the non-solvent is used as an additive, the viscosity of the casting solution is increased, resulting in delayed phase separation during film formation, thereby forming a film structure having a spherical crystal shape. The addition of different additives to the casting solution has different effects on the phase separation thermodynamics and mass transfer kinetics during the film formation process, and the prepared polyvinylidene fluoride (PVDF) hydrophobic microporous membranes are also different.

Nano-silica [23–25] (nSiO_2) is an inorganic non-metallic material with a large specific surface area and a three-dimensional network structure. nSiO_2 is often used to improve the properties of materials and products due to its unique particle size, large specific surface area, good heat resistance and wear resistance, and strong surface adsorption. The surface of nSiO_2 has a large number of hydroxyl groups and unsaturated bonds, which can form hydrogen bonds or chemical bonds with organic polymer materials. When nSiO_2 reacts with a polymer compound due to its special effect, it forms a spatial network structure, thereby improving the mechanical strength and wear resistance of the polymer material. Therefore, nSiO_2 has great value in the modification of the polymer and the improvement of the mechanical strength of the polymer.

However, since the nanoparticles are poorly dispersed when mixed with the polymer material solution, the nanoparticles are easily agglomerated, and the properties of the prepared polymer materials are affected to some extent. In this paper, the PVDF- SiO_2 hydrophobic microporous composite membrane was prepared by in-situ synthesis of nano-silica to solve this problem.

Firstly, tetraethyl orthosilicate (TEOS) was used as the silicon source, and nSiO_2 was synthesized in-situ by sol-gel method. The nSiO_2 sols of different sizes were prepared by controlling the concentration and amount of ammonia in the catalyst. Then, the in-situ synthesized nSiO_2 sol mixed with PVDF to prepare a hydrophobic microporous composite membrane by immersion precipitation phase inversion. Finally, the high-flux, high-porosity, high-hydrophobic PVDF microporous membrane can be obtained under the optimal addition of 20 nm SiO_2 sol and optimal condition of double coagulation bath.

2. Materials and methods

2.1. Materials

PVDF(FR904) was purchased from Shanghai San Ai Fu Xin Material Co., Ltd. N,N-dimethylacetamide was obtained from Shanghai Aladdin Reagent Co., Ltd. Ethyl orthosilicate, phosphoric acid, ethanol, and phosphoric acid were all obtained from Sinopharm Chemical Reagent Co., Ltd., China.

2.2. Preparation of the nSiO_2 sol

Ammonia water and ethanol were placed under ultrasonic vibration to mix well. After a period of time, add TEOS to continue the ultrasonic shock mixing. Subsequently, the mixture was stirred with a constant temperature heating magnetic stirrer to control a certain temperature until the solution became milky white, stirring was stopped. The mixed solution was allowed to stand overnight, and then the nSiO_2 sol was obtained. In this experiment, the morphology and size of nSiO_2 sol particles were controlled by the concentration and content of the catalyst (ammonia). Three sizes of nano-silica (500, 200, and 20 nm) were prepared. The stability and controllability of the preparation method can be demonstrated by the characterization of different size nano silica.

2.3. Characterization of nSiO_2 sol

2.3.1. Scanning electron microscopy observation of nSiO_2 sol

Scanning electron microscopy (SEM) is the most effective and intuitive method to investigate the surface morphology, size, and dispersion of nanoparticles. The prepared nSiO_2 sol was dropped onto a copper piece with a capillary tube and fixed on the sample stage with a conductive paste and subjected to gold spraying treatment, then the sample preparation was completed. Finally, the sample stage was placed under an SEM, and the surface morphology, size, and dispersion of the nSiO_2 sol were observed according to a certain magnification.

The nSiO₂ sol prepared under three different conditions was analyzed. Scanning electron micrographs are shown in Fig. 1.

Fig. 1 is an SEM of the nSiO₂ sol. The observation shows that the morphology of the SiO₂ particles in the nSiO₂ sol synthesized by the sol–gel method is spherical, and the particle size is uniform, the sphere is regular, the dispersion of nSiO₂ particles is good, and there is no agglomeration phenomenon.

2.3.2. Fourier transform infrared spectroscopy spectra of nSiO₂ sol

The variation of the nSiO₂ sol functional group was analyzed by Fourier transform infrared spectroscopy (FTIR). The prepared nSiO₂ sol was, respectively, mixed with potassium bromide powder, vacuum freeze-dried, and uniformly ground, and then the infrared absorption spectrum of the samples were measured by FTIR spectrometer.

The nSiO₂ sols prepared under three different conditions were analyzed. The infrared absorption spectrum is shown in Fig. 2.

Fig. 2 shows the infrared spectrum of nSiO₂. It can be seen from the figure that the nSiO₂ sols prepared by the three methods have the characteristic absorption peak of SiO₂. The 1,093 cm⁻¹ is the antisymmetric stretching vibration peak of Si–O–Si bond, the 800 and 463 cm⁻¹ is the symmetric stretching vibration peak of Si–O bond, the 953 cm⁻¹ is the bending vibration absorption peak of Si–OH bond, the 1,634 cm⁻¹ is the bending vibration peak of H–O–H of water, and the 3,446 cm⁻¹ is the stretching vibration peak of –OH. The nanoparticles prepared by the sol–gel method were verified to be nSiO₂ by infrared spectrum analysis.

2.3.3. X-ray diffraction analysis of nSiO₂ sol

The nSiO₂ was characterized by XRD using a Japanese Society of Science IV combined X-ray diffractometer. Test conditions: CuKα ray, Ni filter, tube voltage 36 kV, tube current 20 mA, scan rate 8°/min, scan range 5°–60°.

The nSiO₂ prepared under three different conditions was analyzed, respectively. X-ray diffraction (XRD) is shown in Fig. 3.

Fig. 3 shows the XRD pattern of the sample. It can be seen from the figure that the nSiO₂ sols prepared by the three methods have a broad peak between 15° and 35°, and the peak value is about 22°. It indicates that the prepared nSiO₂ sol is amorphous. The composition of the substances is the same as the amorphous structure.

2.4. Preparation of PVDF–nSiO₂ composite membrane

The PVDF–nSiO₂ hydrophobic microporous composite membrane was prepared by mixing nSiO₂ sol into casting solution. The nSiO₂ sol was prepared using the situ synthesis method. The effects of different addition levels of 20 nm nSiO₂ sol on the structure and properties of PVDF hydrophobic microporous membranes were investigated.

The PVDF powder was dried in a vacuum oven for 24 h to completely remove moisture from the powder. A certain amount of 20 nm SiO₂ sols was weighed into a

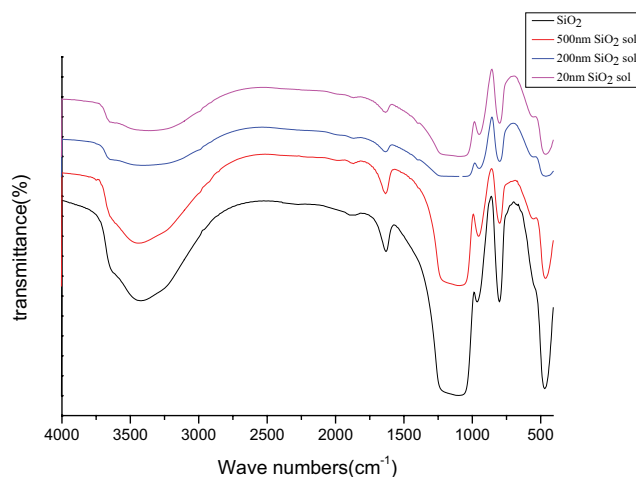


Fig. 2. FTIR spectra of nSiO₂ sols.

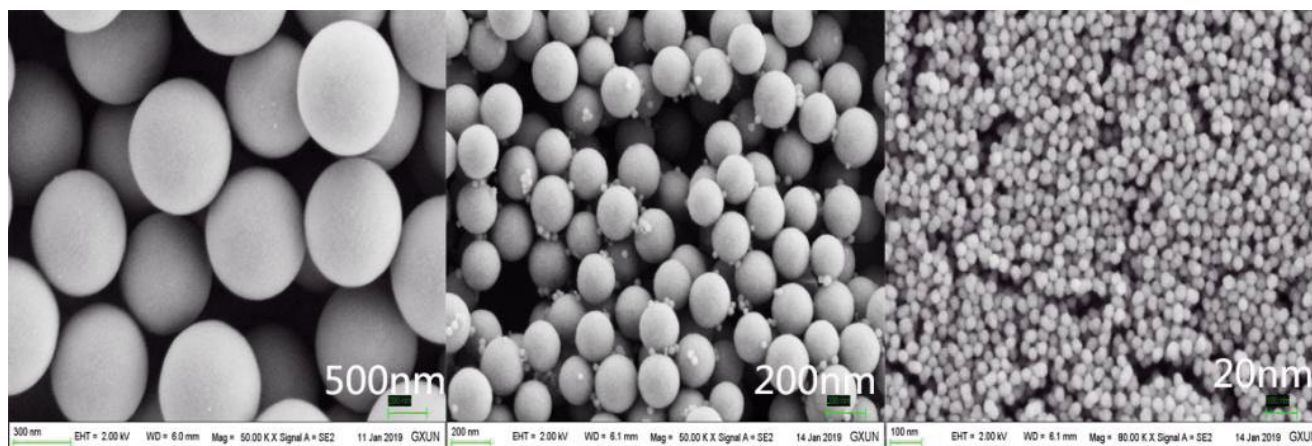


Fig. 1. SEM of nSiO₂ sol.

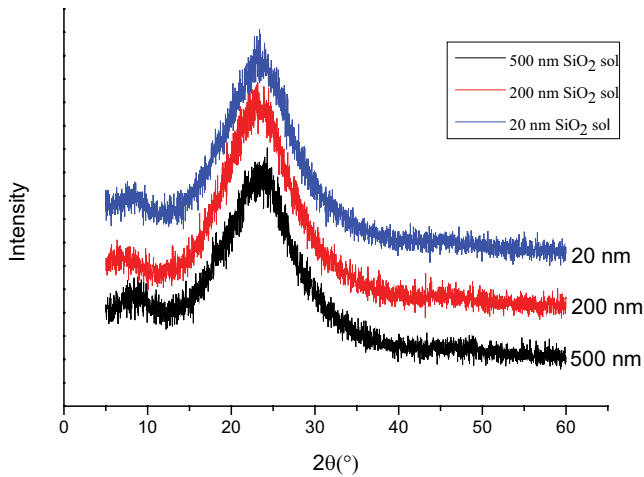


Fig. 3. XRD patterns of different nanoparticles SiO₂ sol.

round bottom flask, DMAc was added, and then the bottom was placed in an ultrasonic cleaner to uniformly disperse the nSiO₂ sol in the solvent. Then, PVDF/phosphoric acid (5%) was added to the round bottom flask, and the round bottom flask was sealed with a rubber stopper. The round bottom flask was placed in a constant temperature heating magnetic stirrer and stirred at 50°C until the casting solution became colorless and transparent. The round bottom flask was subjected to defoaming treatment in a vacuum drying oven, and the bubbles in the casting solution were completely removed. Pour the casting solution onto the glass plate at room temperature and scrape it into a thin layer with a self-made glass rod. Leave it in the air at room temperature for about 10 s. Then, immerse the glass plate in 50°C deionized water and form a film of the casting solution. After the glass plate was detached, the membrane was taken out and immersed in deionized water for 2 d. The water was exchanged at intervals with the solvent and additives during this period to completely remove the residual solvent and additives in the film. After soaking, the membrane was taken out and dries at room temperature. The composition of the casting solution is shown in Table 1.

2.5. Membrane structure and performance characterizations

2.5.1. Determination of porosity of the membrane

The porosity calculation of the film generally uses the dry-wet weight method. First, a sample of a certain size was cut from the prepared film, placed in a beaker containing ultrapure water, and ultrasonically shaken for 2 h to ensure that the pores of the film were filled with water. The film sample was taken out. The water on the surface of the film was sucked up with a filter paper. Weighed and recorded it. The sample was then placed in an oven at 80°C overnight until constant weight. Weighed and counted by an electronic balance. Calculated as follows:

$$\varepsilon = \frac{(m_n - m_p) / \rho_n}{(m_n - m_p) / \rho_n + m_p / \rho_p} \quad (1)$$

Table 1
Composition of casting solution

Additive (20 nm SiO ₂ sol)/mL	Additive (phosphoric acid)/%	DMAc	PVDF
0	5%	80%	15%
1	5%	80%	15%
2	5%	80%	15%
3	5%	80%	15%
4	5%	80%	15%
5	5%	80%	15%
6	5%	80%	15%

In the formula, ε is the porosity of the film; m_n is the wet film mass of the water immersed; m_p is the mass of the dry film; ρ_n is the density of water; ρ_p is the density of the PVDF powder.

2.5.2. Mean pore size measurement of the membrane

The average pore size of the membrane was calculated using the filtration rate method. First, a PVDF membrane of a certain size was cut out, fixed on an ultrafiltration cup, and the volume of ultrapure water permeating through the membrane was measured under a pressure of 0.1 Mpa to calculate the filtration rate. The average pore size was calculated using the modified formula of Ye Lingbi. Calculated as follows:

$$r_f = \sqrt{\frac{(2.9 - 1.75\varepsilon)8\eta l Q}{\varepsilon \cdot P \cdot A}} \quad (2)$$

In the formula, ε is the porosity of the film; η is the viscosity of water; l is the average thickness of the film; A is the area of the film; Q is the filtration rate; P is the operating pressure; r_f is the average pore diameter.

2.5.3. Determination of membrane pure water flux

The pure water flux of the membrane is typically measured using a cup ultrafilter. The membrane was placed in an ultrafiltration cup, and the membrane was compacted with ultrapure water for 30 min under a pressure of 0.1 MPa. After the flow rate was stabilized, the volume of ultrapure water permeating through the membrane was recorded for a certain period of time. Calculated as follows:

$$J = \frac{V}{(A \cdot t)} \quad (3)$$

In formula, V is the permeate volume of water; t is the test time; A is the effective membrane area.

2.5.4. Membrane flux measurement

Membrane flux was measured using direct contact membrane distillation (DCMD) device, as shown in Fig. 4.

A membrane of suitable size was cut and placed on the membrane module. Three percent of sodium chloride solution is treated with this membrane in DCMD device. The experiment conditions were as follows: the temperature of the hot side salt liquid was 60°C, the temperature of the cold side water was 20°C, the flow rate of the hot side liquid was 96 L/h, and the flow rate of the cold side solution was 80 L/h. The mass change of the solution in the hot side liquid tank, Δm , was recorded every 20 min. In the meantime measure, the change in conductivity of the cold side solution. The membrane flux calculation formula is as follows:

$$N = \frac{\Delta m}{(A \cdot t)} \quad (4)$$

In the formula, N is the membrane flux, A is the effective area of the membrane, and t is the time.

2.5.5. SEM observation of membrane

SEM is the most effective and intuitive way to observe the surface and internal structure of a membrane. Firstly, the microporous membrane is subjected to liquid nitrogen treatment, and the membrane is carefully broken to form a flat membrane cross-section. Then, the selected membrane section and the surface sample are respectively fixed and sprayed with gold. Finally, the sample stage is placed under an SEM, and different magnifications are selected to observe the microstructure of the surface and section of the film.

2.5.6. Membrane wettability

The wettability of the PVDF microporous membrane was usually characterized by a static pure water contact angle (CA). The contact angle of the PVDF membrane was tested in the experiment using a JY-82B video contact angle

meter. Each film was repeatedly measured five times with different points, and the average value was calculated as the measured contact angle.

3. Results and discussion

3.1. Effect of different additions $n\text{SiO}_2$ sol on film porosity and average pore size

The effects of different additions $n\text{SiO}_2$ sol on porosity, average pore size, pure water flux, and membrane flux were investigated during the experiment. As shown in Figs. 5 and 6.

3.2. Effect of different additions $n\text{SiO}_2$ sol on membrane flux and pure water flux

The conductivity of the cold side solution was measured. As shown in Fig. 7, for the different addition $n\text{SiO}_2$ sol, the conductivity of the cold side solution was changed with time.

It can be seen from Fig. 5 that as the content of $n\text{SiO}_2$ sol added in-situ increases, the porosity and average pore size of the PVDF film increase first and then decrease. The film prepared by adding the $n\text{SiO}_2$ sol has a larger porosity and average pore diameter than that which is not added. When the SiO_2 sol is added in an amount of 5 mL, the porosity is at the most value 75%. When the SiO_2 sol is added in an amount of 2 mL, the average pore diameter reaches a maximum of 0.8 μm . As can be seen from the figure, the addition of the $n\text{SiO}_2$ sol increases the porosity and average pore size of the film.

It can be seen from Fig. 6 that as the content of $n\text{SiO}_2$ sol is increase, the pure water flux and membrane flux of the PVDF membrane also tend to increase first and then decrease. When the amount of $n\text{SiO}_2$ sol added is 5 mL, the membrane flux reaches the highest value of 31.02 $\text{kg m}^{-2} \text{h}^{-1}$, and the pure water flux reaches the maximum of 165.6 $\text{L m}^{-2} \text{h}^{-1}$. It is known from Fig. 7 that the conductivity of the cold side solution gradually decreases

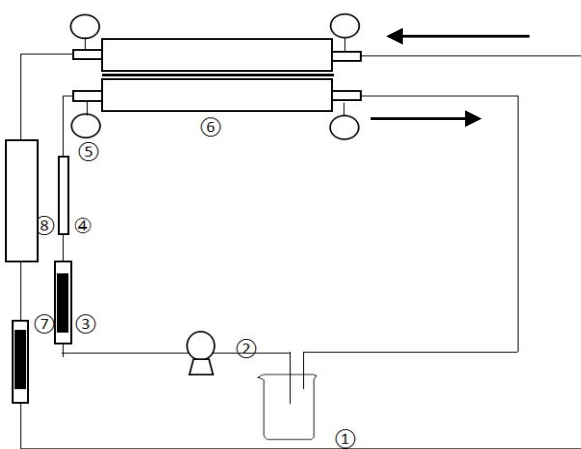


Fig. 4. The flow chart of direct contact membrane distillation experiment (1) sink, (2) circulating pump, (3) flow meter, (4) heater, (5) thermometer, (6) membrane assembly, (7) flow meter, and (8) chiller.

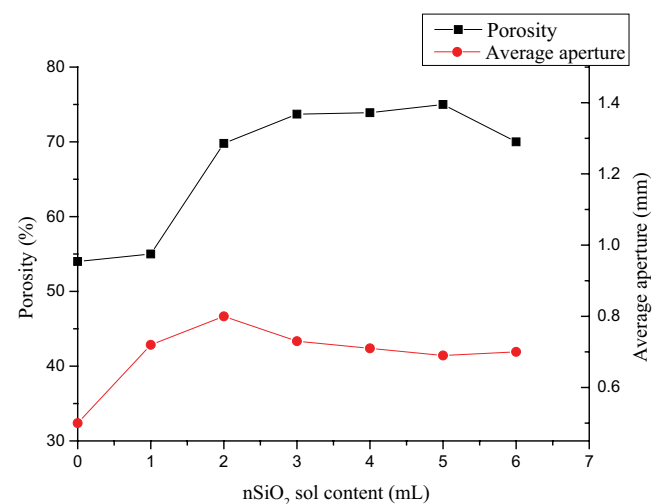


Fig. 5. Effect of different additions $n\text{SiO}_2$ sol on film porosity and average pore size.

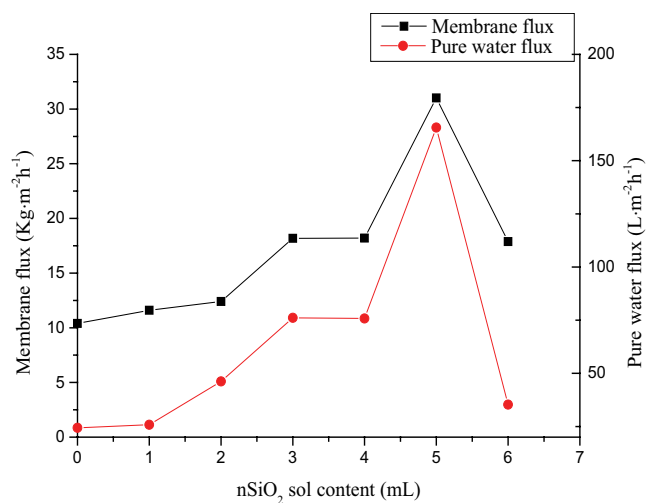


Fig. 6. Effect of different additions nSiO₂ sol on membrane flux and pure water flux.

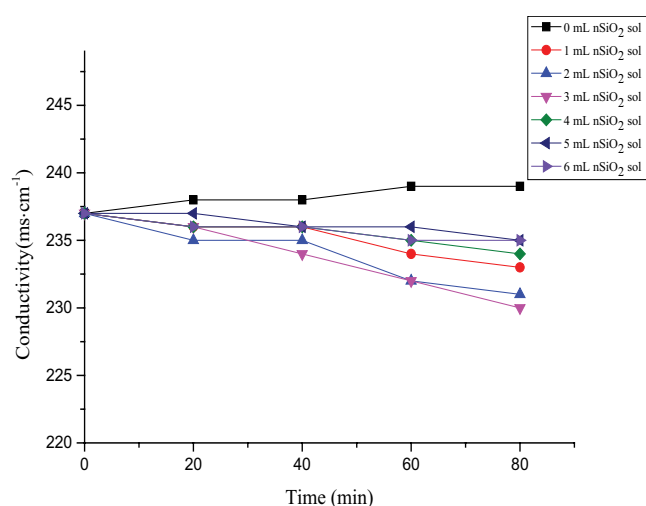


Fig. 7. Change in conductivity of the cold side solution.

during the membrane distillation process, when it used the PVDF composite membrane modified by in-situ synthesized nSiO₂ sol. It is indicated that the prepared membrane has a high rejection rate of sodium chloride, and only allows water molecules to pass, so that the conductivity of the cold side solution decreases.

Since the prepared nSiO₂ sol was not further processed, it contains a large amount of silanol groups, and it can be regarded as a porogen and added to the casting solution. Moreover, the addition of nSiO₂ sol changes the viscosity of the original casting solution. When the amount of nSiO₂ sol added is small, the liquid–liquid phase separation dominates during the film formation process, which accelerates the exchange rate between the solvent and the non-solvent and increases the porosity of the film. When the content of nSiO₂ sol is increased, the viscosity of the casting solution increases. The solid–liquid phase separation dominates the delayed phase processes, resulting in a decrease in the porosity and average pore size of the membrane.

3.3. Comparison of membrane structure

The structure of the PVDF membrane prepared by six different additions of nSiO₂ sol was analyzed by SEM to observe the surface and cross-sectional structure of the membrane. Electron micrographs are shown in Figs. 8 and 9.

As can be seen from the surface maps of Fig. 8, the surface is composed of a relatively uniform and loose network-like porous structure. And the surface of the film forms a micro-nano structure, which enhances the roughness of the film and thereby increases the hydrophobicity of the film. It can be seen from the figures when the content of the nSiO₂ sol is 5 mL, the pores on the surface of the membrane are dense, which is consistent with the calculated porosity of the membrane. As can be seen from the sectional view of Fig. 9, the sections are all asymmetric structures. It is an asymmetric structure consisting of a layer of surface cortex, finger-like pores, and sponge-like structure. When the content of nSiO₂ sol is 5 mL, the pore structure of the membrane is more, and the structure of the finger pore is beneficial to improve the permeability of the membrane, so the membrane flux and pure water flux are improved.

3.4. Membrane wettability

The wetting properties of the film were characterized using a static pure water contact angle (CA). The contact angles of the PVDF films containing different addition of nSiO₂ sol were tested using a JY-82B video contact angle meter. As shown in Fig. 10.

It can be seen from Fig. 10 that the PVDF composite membrane modified by in-situ synthesized nSiO₂ sol has good hydrophobicity. However, as the content of nSiO₂ sol added increases, the contact angle of the film decreases. This may be because nSiO₂ contains silanol groups. It leads to increased hydrophilicity as the content of nSiO₂ sol increases. When nSiO₂ sol added to the casting solution, it not only increases the viscosity of the casting solution but during the phase inversion process, a small portion fails to be converted into a non-solvent. As the content of the nSiO₂ sol increases, the amount of nSiO₂ remaining in the film also increases, so that the contact angle of the film becomes small. Compare to the contact angle of 92.7° prepared with phosphoric acid as an additive, the hydrophobic property of PVDF-nSiO₂ composite membrane have a significant improvement.

3.5. Optimization of PVDF-nSiO₂ composite membrane preparation process

In order to get better membrane separating property, the double coagulation bath method was employed to further improve the film-forming process. In the previous experimental work, the optimal dual coagulation bath operating conditions obtained by orthogonal experiments were: the first coagulation bath was 60°C 40% ethanol, soaked for 20 s, and the second coagulation bath was 60°C ultrapure water. The PVDF powder was dried in a vacuum oven for 24 h to completely remove moisture from the powder. Five milliliters of nSiO₂ sol was weighed into a round bottom flask, and DMAc was added. The bottom was placed in an

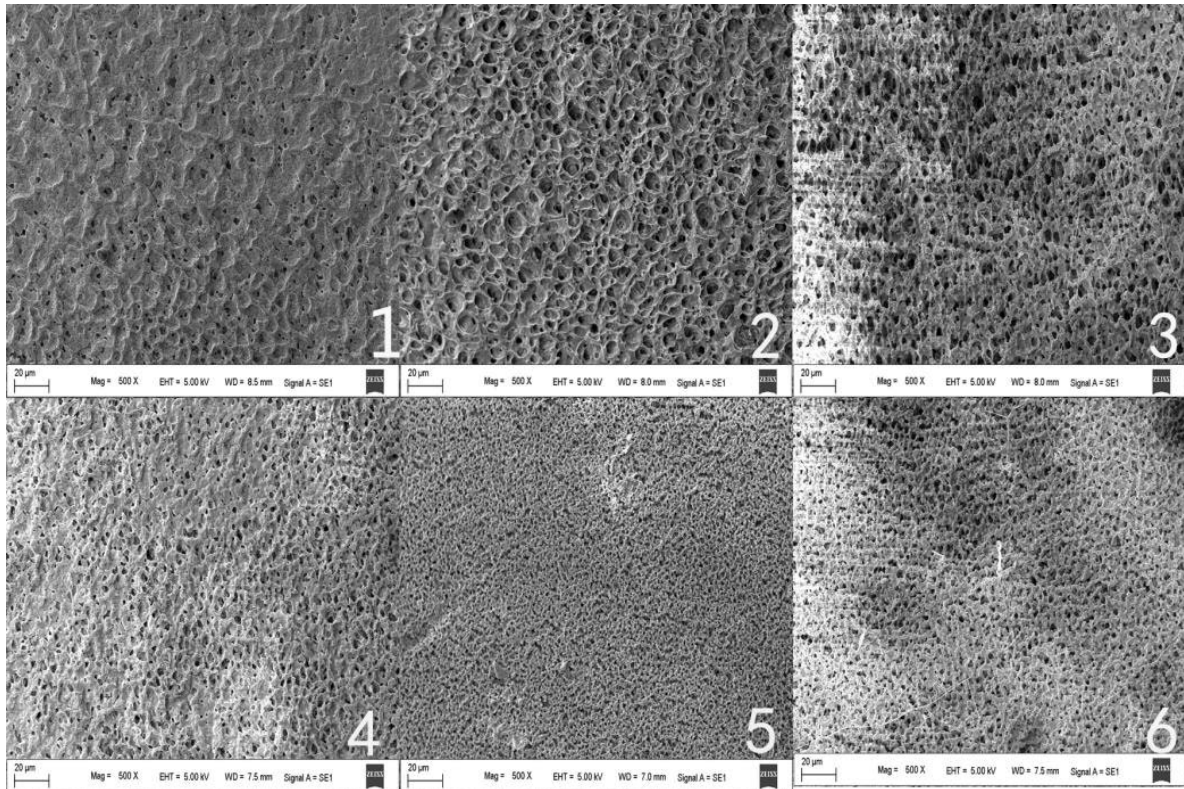


Fig. 8. Surface electron micrograph of different content of nSiO₂ sol (nSiO₂ sol (1) 1 mL, (2) 2 mL, (3) 3 mL, (4) 4 mL, (5) 5 mL, and (6) 6 mL).

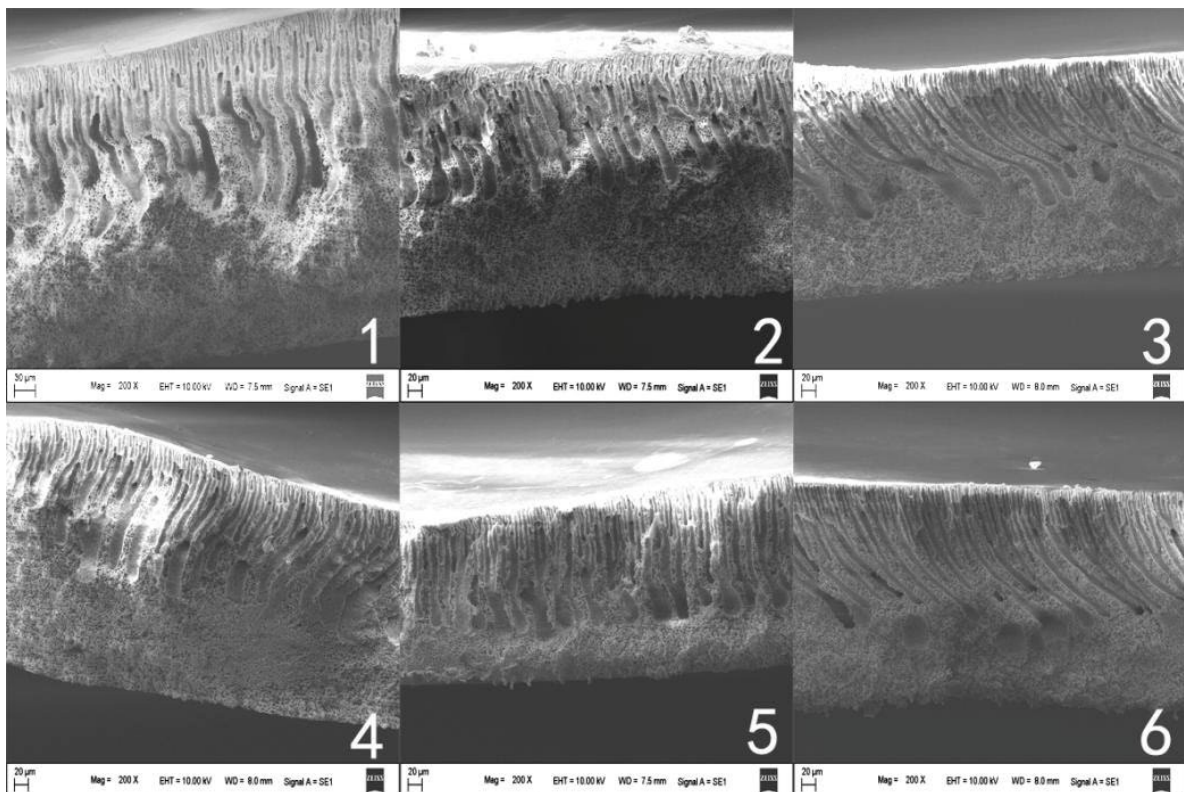


Fig. 9. Electron micrograph of cross section of different content of nSiO₂ sol (nSiO₂ sol (1) 1 mL, (2) 2 mL, (3) 3 mL, (4) 4 mL, (5) 5 mL, and (6) 6 mL).

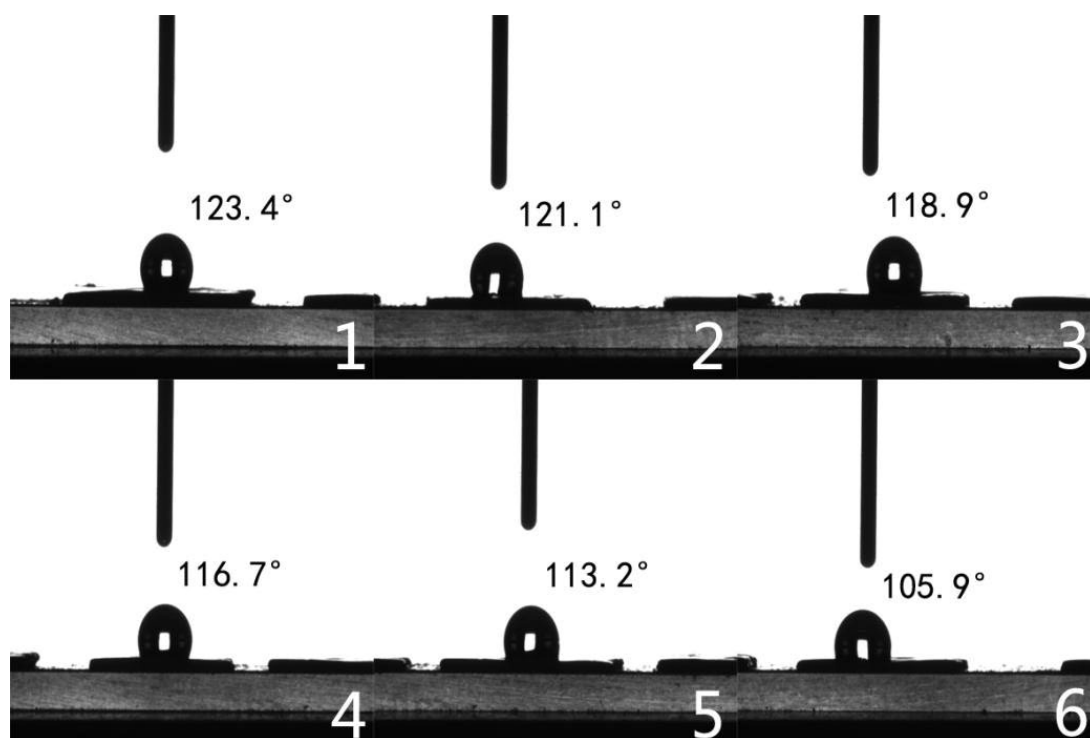


Fig. 10. Contact angle of film prepared by different content of $n\text{SiO}_2$ sol ($n\text{SiO}_2$ sol (1) 1 mL, (2) 2 mL, (3) 3 mL, (4) 4 mL, (5) 5 mL, and (6) 6 mL).

ultrasonic cleaner to uniformly disperse the $n\text{SiO}_2$ sol into the solvent. Then, PVDF/phosphoric acid (5%) was added to the round bottom flask, and the round bottom flask was sealed with a rubber stopper. The round bottom flask was placed in a constant temperature heating magnetic stirrer and stirred at 50°C until the casting solution became colorless and transparent. The round bottom flask was subjected to defoaming treatment in a vacuum drying oven. When the bubbles were completely removed, the casting solution was taken out for use. Pour the casting solution onto the glass plate at room temperature and scrape it into a thin layer with a self-made glass rod. Leave it in the air at room temperature for a certain period of time. The glass plate was immersed in 40% ethanol at 60°C for 20 s and then placed it at 60°C ultrapure water. After detachment from the glass plate, the film is taken out and immersed in deionized water for 2 d. At this interval, water is exchanged to completely remove the residual solvent and additive in the film. After soaking, take out and dry the film at room temperature.

The prepared film was characterized. The performances are shown in Table 2.

It can be seen from Table 2 that the double coagulation bath method was employed to prepare the $n\text{SiO}_2$ -PVDF composite membrane, the membrane flux porosity and membrane wettability are greatly improved. The structure and morphology of PVDF hydrophobic microporous composite membrane were optimized by the double coagulation bath method, and the performance of the membrane was greatly improved.

The optimized film was characterized for structure and wetting properties, as shown in Fig. 11.

As can be seen from Fig. 11, the surface of the membrane is composed of a relatively uniform and loose network-like porous structure. The bottom surface is a haw-like undulating structure, and the roughness of the film surface is to increase the hydrophobicity of the film. The cross-section of the membrane is an asymmetric structure consisting of a thin surface cortex, finger-like pores, and a sponge-like structure. It can be seen from the sectional view that the sponge structure of the membrane is small, and there are many finger holes, so that the resistance of the gas permeating the membrane is reduced, and the membrane flux is increased.

Table 2
Performance parameters of PVDF membrane

Membrane performance	Membrane flux ($\text{kg m}^{-2} \text{h}^{-1}$)	Porosity (%)	Average pore diameter (μm)	Membrane wettability ($^\circ$)
Optimized membranes	42.7	78.7	0.57	127.3
Not optimized membranes	31.02	75	0.7	113.2

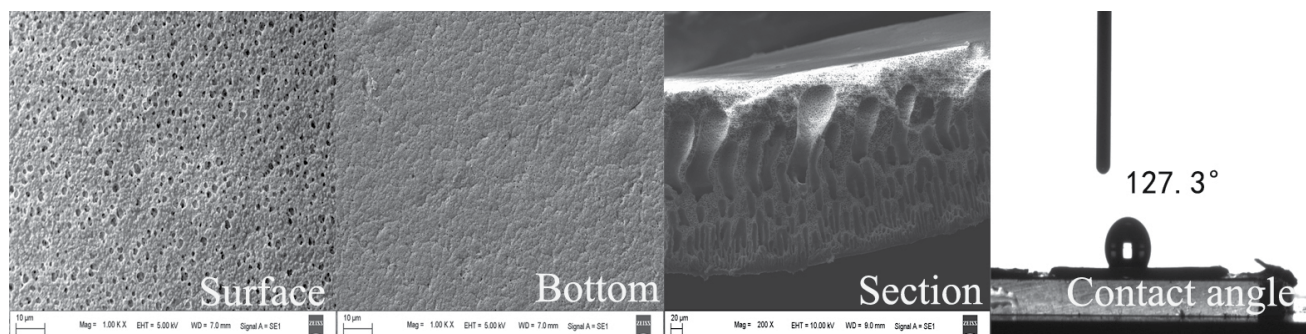


Fig. 11. Optimization of electron microscope and contact angle of double coagulation bath method.

4. Conclusions

In this paper, the $n\text{SiO}_2$ sol was synthesized in-situ by sol-gel method. The spherical SiO_2 sol at different size was prepared by changing the concentration and content of ammonia in the catalyst to control the morphology and size of the $n\text{SiO}_2$ sol particles. The effect of 20 nm SiO_2 sol on the structure and properties of PVDF hydrophobic microporous membrane was investigated.

By performing infrared absorption spectroscopy on the prepared $n\text{SiO}_2$ sol, it was found that the prepared nanoparticles all have characteristic absorption peaks of SiO_2 . Moreover, the prepared $n\text{SiO}_2$ sol particles have uniform size, spherical regularity, good dispersion of nanoparticles, and no agglomeration between particles. The prepared $n\text{SiO}_2$ sol was subjected to XRD diffraction analysis, and it was found that the $n\text{SiO}_2$ sol prepared by the three methods was composed of an amorphous substance and belonged to an amorphous structure.

The $n\text{SiO}_2$ sol synthesized in-situ can improve the properties and structure of the membrane by mixing it into the casting solution. When the $n\text{SiO}_2$ sol added is 5 mL, the pure water flux of the membrane is $165.6 \text{ L m}^{-2} \text{ h}^{-1}$, and the membrane flux is $31.02 \text{ kg m}^{-2} \text{ h}^{-1}$, which is the highest. The porosity of the membrane is the highest 75% and the average pore diameter of the membrane was $0.7 \mu\text{m}$. On this basis, the double coagulation bath method was employed to further improve the film-forming process. The properties and structure of the membrane were optimized. The membrane flux was $42.7 \text{ kg m}^{-2} \text{ h}^{-1}$ and the porosity was 78.7%. The performance and structure of the membrane were optimized compared with the direct addition of $n\text{SiO}_2$. The PVDF hydrophobic microporous composite membrane prepared by a double coagulation bath method can obtain a high membrane flux and high porosity.

Acknowledgments

This research was supported by the National Natural Science Foundation of China (No. 21566007), (No. 21968008), and (No. 21466008), and the Guangxi Natural Science Foundation (2018GXNSFAA050025).

References

- [1] A. Alkhudhiri, N. Darwish, N. Hilal, Membrane distillation: a comprehensive review, *Desalination*, 287 (2012) 2–18.

- [2] A. Khalifa, H. Ahmad, M. Antar, T. Laoui, M. Khayet, Experimental and theoretical investigations on water desalination using direct contact membrane distillation, *Desalination*, 404 (2017) 22–34.
- [3] P. Wang, T.S. Chung, Recent advances in membrane distillation processes: membrane development, configuration design and application exploring, *J. Membr. Sci.*, 474 (2015) 39–56.
- [4] A. Luo, N. Lior, Study of advancement to higher temperature membrane distillation, *Desalination*, 419 (2017) 88–100.
- [5] M. Khayet, Membranes and theoretical modeling of membrane distillation: a review, *Adv. Colloid Interface Sci.*, 164 (2011) 56–88.
- [6] A.M. Alklaibi, N. Lior, Membrane-distillation desalination: status and potential, *Desalination*, 171 (2005) 111–131.
- [7] D. Singh, K.K. Sirkar, Performance of PVDF flat membranes and hollow fibers in desalination by direct contact membrane distillation at high temperatures, *Sep. Purif. Technol.*, 187 (2017) 264–273.
- [8] D. Zhao, J. Zuo, K.J. Lu, T.S. Chung, Fluorographite modified PVDF membranes for seawater desalination via direct contact membrane distillation, *Desalination*, 413 (2017) 119–126.
- [9] L. Francis, N. Ghaffour, A.S. Al-Saadi, G.L. Amy, Submerged membrane distillation for seawater desalination, *Desal. Water Treat.*, 55 (2014) 2741–2746.
- [10] V.D. Alves, I.M. Coelho, Orange juice concentration by osmotic evaporation and membrane distillation: a comparative study, *J. Food Eng.*, 74 (2006) 125–133.
- [11] S. Gunko, S. Verbych, M. Bryk, N. Hilal, Concentration of apple juice using direct contact membrane distillation, *Desalination*, 190 (2006) 117–124.
- [12] M.B. Jensen, K.V. Christensen, R. Andréen, L.F. Sørensen, B. Norddahl, A model of direct contact membrane distillation for black currant juice, *J. Food Eng.*, 107 (2011) 405–414.
- [13] F. Banat, S. Al-Asheh, M. Qtaishat, Treatment of waters colored with methylene blue dye by vacuum membrane distillation, *Desalination*, 174 (2005) 87–96.
- [14] J. Li, Y. Guan, F. Cheng, Y. Liu, Treatment of high salinity brines by direct contact membrane distillation: effect of membrane characteristics and salinity, *Chemosphere*, 140 (2015) 143–149.
- [15] P.M. Kamrani, O. Bakhtiari, P. Kazemi, T. Mohammadi, Theoretical modeling of direct contact membrane distillation (DCMD): effects of operation parameters on flux, *Desal. Water Treat.*, 56 (2014) 2013–2022.
- [16] E.K. Oikonomou, S. Karpati, S. Gassara, A. Deratani, F. Beaume, O. Lorain, S. Tencé-Girault, S. Norvez, Localization of antifouling surface additives in the pore structure of hollow fiber PVDF membranes, *J. Membr. Sci.*, 538 (2017) 77–85.
- [17] S.H. Park, Y. Ahn, M. Jang, H.J. Kim, K.Y. Cho, S.S. Hwang, J.H. Lee, K.Y. Baek, Effects of methacrylate based amphiphilic block copolymer additives on ultra filtration PVDF membrane formation, *Sep. Purif. Technol.*, 202 (2018) 34–44.
- [18] S. Arefi Oskoui, V. Vatanpour, A. Khataee, Effect of different additives on the physicochemical properties and performance of NLDH/PVDF nanocomposite membrane, *Sep. Purif. Technol.*, 209 (2019) 921–935.

- [19] R. Zhou, D. Rana, T. Matsuura, C.Q. Lan, Effects of multi-walled carbon nanotubes (MWCNTs) and integrated MWCNTs/SiO₂ nano-additives on PVDF polymeric membranes for vacuum membrane distillation, *Sep. Purif. Technol.*, 217 (2019) 154–163.
- [20] B. Yang, X. Yang, B. Liu, Z. Chen, C. Chen, S. Liang, L.Y. Chu, J. Crittenden, PVDF blended PVDF-g-PMAA pH-responsive membrane: effect of additives and solvents on membrane properties and performance, *J. Membr. Sci.*, 541 (2017) 558–566.
- [21] W. Zhang, Y.M. Zhang, R. Fan, R. Lewis, A facile TiO₂/PVDF composite membrane synthesis and their application in water purification, *J. Nanopart. Res.*, 18 (2016) 31–41.
- [22] N. Meng, R.C.E. Priestley, Y. Zhang, H. Wang, X. Zhang, The effect of reduction degree of GO nanosheets on microstructure and performance of PVDF/GO hybrid membranes, *J. Membr. Sci.*, 501 (2016) 169–178.
- [23] H.L. Shen, H. Liao, C.F. Xiao, Formation mechanism and properties of polyvinylidene fluoride (PVDF)/nano-silica hybrid membranes, *Adv. Mater. Res.*, 123–125 (2010) 93–96.
- [24] M. Zhao, Z.Z. Ren, M.B. Yang, W. Yang, Effects of modified nano-silica on the microstructure of PVDF and its microporous membranes, *J. Polym. Res.*, 26 (2019) 28–40.
- [25] W.F. Yang, Z.Q. Zhang, Z.Y. Gu, X.X. Shen, Q.F. Zhang, Research on the superhydrophobic modification of polyvinylidene fluoride membrane, *Adv. Mater. Res.*, 197–198 (2011) 514–517.